International Journal of Engineering Sciences & Research Technology

(A Peer Reviewed Online Journal)
Impact Factor: 5.164

IJESRT

Website: www.ijesrt.com Mail: editor@ijesrt.com

Correspondence Address: 116, Sukhdev Nagar Ext-1, Airport Road, Indore – 452005, Madhya Pradesh, INDIA

RESEARCHERID
THOMSON REUTERS

[Lankouande* *et al.*, 12(8): August, 2023]
IC™ Value: 3.00

ISSN: 2277-9655
Impact Factor: 5.164
CODEN: IJESS7

IJESRT

INTERNATIONAL JOURNAL OF ENGINEERING SCIENCES & RESEARCH TECHNOLOGY

NUMERICAL SIMULATION OF THE AIR FLOW IN AN INDIRECT SOLAR DRYER WITH NATURAL CONVECTION

Roland LANKOUANDE[*1], G. Gilbert NANA[2], Souleymane OUEDRAOGO[2], Kalifa PALM[3], Sié KAM[2], Frédéric OUATTARA[1]

[1]Laboratoire de Chimie Analytique et de Physique Spatiale et Énergétique (LACAPSE), Université Norbert ZONGO, BP 376 Koudougou, Burkina Faso.

[2]Laboratoire d'Energies Thermiques Renouvelables (LETRE), Université Joseph KI-ZERBO, 03 BP 7021 Ouagadougou 03, Burkina Faso.

[3]Institut de Recherche en Sciences Appliquées et Technologies (IRSAT), 01 BP 7047 Ouagadougou 01, Burkina Faso

Corresponding Author Mail : rolandlankouande@yahoo.fr

DOI: 10.5281/zenodo.8310988

ABSTRACT

In this work, we have simulated the air flow in an indirect solar dryer with natural convection, and we study the behavior of its flow from the inlet of the collector to the outlet of the drying chamber. This phenomenon is governed by the Navier-Stokes equations. These equations, coupled with the initial and boundary conditions, are discretized by a finite difference method and then solved numerically using Gaussian algorithms. The resolution of these equations allows us to have the temperature profile which varies from 303 K to 343 K, also a velocity profile which is between 0.5 m/s and 2.5 m/s and finally a drop in pressure along the drying chamber. Also, we have shown the influence of the geometry of the dryer on the flow of the drying air.

KEYWORDS: Navier-Stokes equations, Gaussian algorithms, temperatures, velocities, pressure

1. INTRODUCTION

Worldwide, around a third of the edible portion of food from seasonal harvests intended for human consumption is lost or wasted [1].

Drying is one of the oldest methods of preservation. But over time, drying techniques have developed, depending on whether you're drying very water-rich agri-food products or seeds [2],[3].

It has been known for decades that the quality of food products is best preserved when they are packaged in an environment whose parameters, such as temperature, speed and (relative) humidity of the drying air, as well as ambient pressure, are controlled [4].

In our study, we will analyze the characteristics of the drying air through a prototype indirect dryer with natural convection (vacuum).

2. MATERIALS AND METHODS

2.1 Materials

Our study focuses on natural air convection in an indirect solar dryer. The prototype used for our study has the following characteristics (fig. 1) :

At the bottom, we have our flat-plate collector (circular in shape, 1.50 m in diameter and 10 cm thick), which is the hot-air production unit. The absorber heats up under the effect of solar radiation. The greenhouse effect

ISSN: 2277-9655
Impact Factor: 5.164
CODEN: IJESS7

produced raises the temperature of the air in the flat plate collector. This air arrives at the inlet of the drying chamber (cylindrical in shape, 0.50 m in diameter and 1.30 m high), passes through it and is then discharged at the top.

Air flow is translated by the continuity equation, the Navier-Stockes equations (conservation of momentum equations) and the conservation of energy equation.

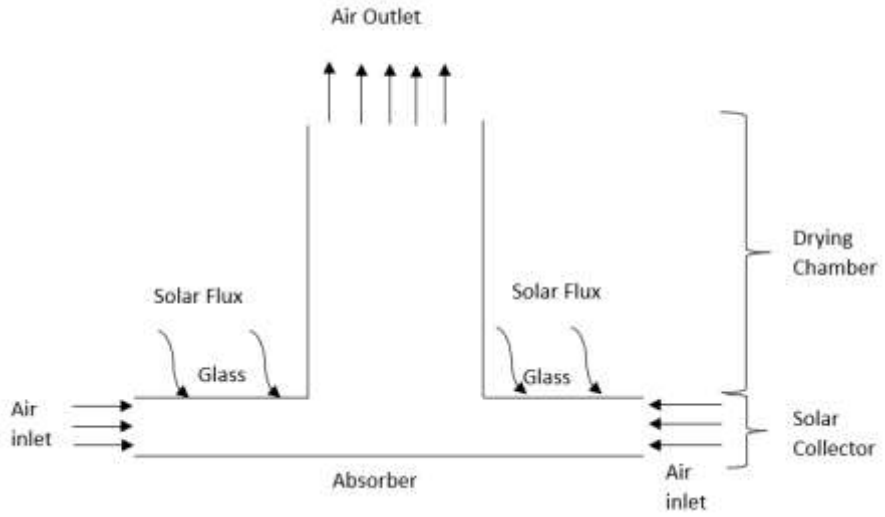

Fig. 1: Schematic diagram of the prototype solar dryer

2.2 Methods

2.2.1 Hypotheses

- The Fluid is viscous and Newtonian
- The flow is considered permanent and laminar
- The system has an axis of symmetry
- Gravity is the only external force
- The properties of the fluid are assumed to be constant.
- The equation for the momentum of air obeys the Boussinesq approximation [5],[6]. This approximation is based on two hypotheses :

1. The density of the fluid is considered constant except in the term ρg
2. The temperature differences are small enough that, in evaluating ρg, we can be satisfied with the first term of ρ as a function of temperature, i.e.

$$\rho = \rho_0[1 - \beta(T - T_0)]$$

Where g= intensity of gravity; ρ =Density of air ; ρ_0= Density of air at reference temperature ; T=Air temperature ; T_0 =air reference temperature ; β = Coefficient of expansion at constant pressure.

2.2.2 Equations

In cylindrical coordinates, we have the following equations :

-Equation of continuity :

ISSN: 2277-9655
Impact Factor: 5.164
CODEN: IJESS7

$\frac{1}{r}\frac{\partial(r\rho V_r)}{\partial r}+\frac{\partial \rho V_z}{\partial z}=0$ (i)

Where r=radial coordinate; z=vertical coordinate; V_r= Radial component of velocity ; V_z= Vertical component of velocity.

-Equation of Energy :

$$\rho Cp\left(V_r\frac{\partial T}{\partial r}+V_z\frac{\partial T}{\partial z}\right)=\lambda\left[\frac{\partial^2 T}{\partial r^2}+\frac{\partial^2 T}{\partial z^2}+\frac{1}{r}\frac{\partial T}{\partial r}\right] \quad \text{(ii)}$$

Where Cp= Calorific capacity at constant pressure ; λ= Thermal conductivity

- Equations of momentum :
  - Radial axis component (Or) :

$$\rho\left(V_r\frac{\partial V_r}{\partial r}+V_z\frac{\partial V_r}{\partial z}\right)=-\frac{\partial P}{\partial r}+\mu\left[\frac{\partial^2 V_r}{\partial r^2}+\frac{1}{r}\frac{\partial V_r}{\partial r}-\frac{V_r}{r^2}+\frac{\partial^2 V_r}{\partial z^2}\right] \quad \text{(iii)}$$

  - Vertical axis component (Oz) :

$$\rho\left(V_r\frac{\partial V_z}{\partial r}+V_z\frac{\partial V_z}{\partial z}\right)=-\frac{\partial P}{\partial z}+\mu\left[\frac{\partial^2 V_z}{\partial r^2}+\frac{\partial^2 V_z}{\partial z^2}+\frac{1}{r}\frac{\partial V_z}{\partial r}\right]-\rho g \quad \text{(iiii)}$$

Where μ= Dynamic viscosity ; P=Pressure

2.2.3 Boundary and initial conditions

To simplify the flow of air through the system, the initial and boundary conditions are as follows : [7],[8] :

-Collector inlet *:*

$V_r=V_{r0}$, $V_z=0$, T=T_0 , P=P_0

With $V_{ro}=0{,}5\ m/s$; T_0=303,15 K (30°C) ; P_0=1 Atm

-On the Absorber:

$V_r=0$, $V_z=0$, T=Tp

With Tp=343,15 K (70°C)

-On the glass *:*

$V_r=0$, $V_z=0$, T=Tv

Tv= (solar flux =600 W/m²)

-On the chimney wall *:*

$V_r=0$, $V_z=0$, $\frac{\partial T}{\partial r}=0$

-At the chimney outlet :

ISSN: 2277-9655
Impact Factor: 5.164
CODEN: IJESS7

$\frac{\partial V_r}{\partial z} = 0, \quad \frac{\partial V_z}{\partial z} = 0, \quad \frac{\partial T}{\partial z} = 0$

-On the axis of symmetry :

$V_r = 0 \ , \ \frac{\partial V_z}{\partial r} = 0, \quad \frac{\partial T}{\partial r} = 0$

Equations (i), (ii), (iii) and (iiii) and their associated initial and boundary conditions are discretised using a finite difference method. The resulting systems of algebraic equations are solved using Gaussian algorithms.

3. RESULTS AND DISCUSSION

The various simulation results were obtained using Comsol 5.3a software.

3.1 Velocity Profile

Fig. 2 shows the evolution of air velocity in 3D (case a) and 2D (case b) in the solar dryer.

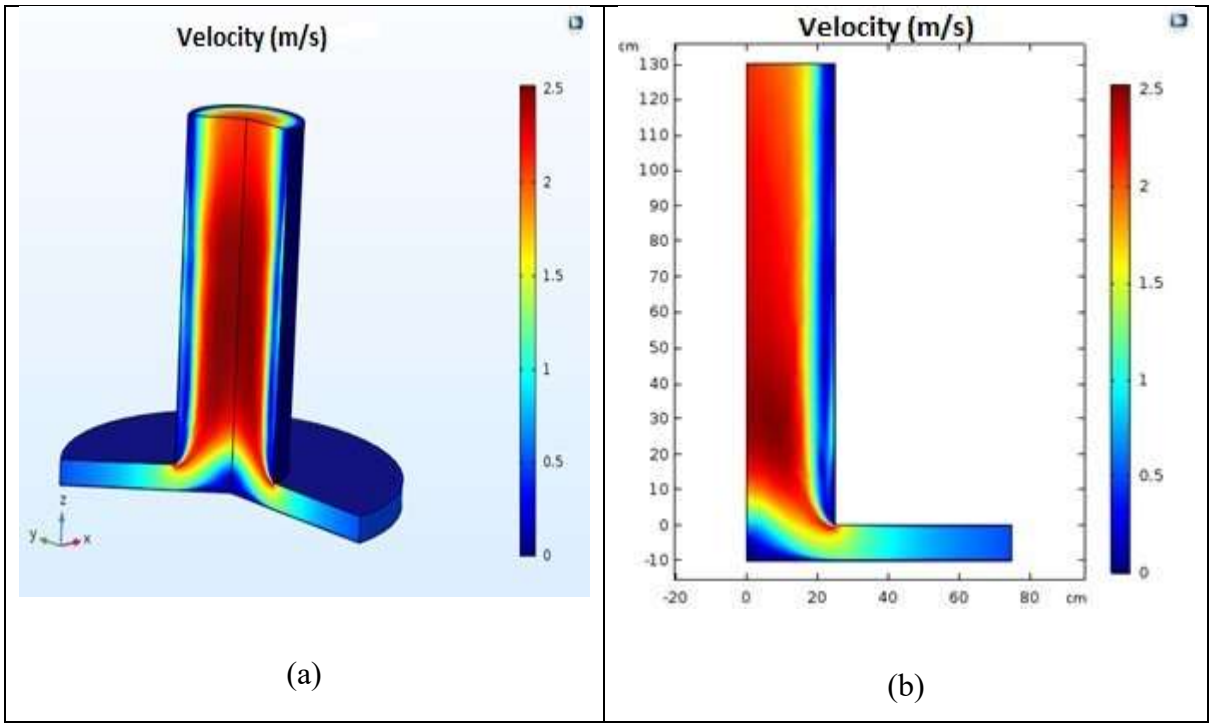

Fig. 2: 3D/2D velocity profiles of the solar dryer

ISSN: 2277-9655
Impact Factor: 5.164
CODEN: IJESS7

Initially, the air velocity at the collector inlet is assumed to be 0.5 m/s. We observe an increase in this speed (up to 2.3 m/s) at the collector outlet / drying chamber inlet. There is a decrease in the cross section airflow. This is the venturi effect.

Fig. 3 shows the 1D velocity at different cross-sections.

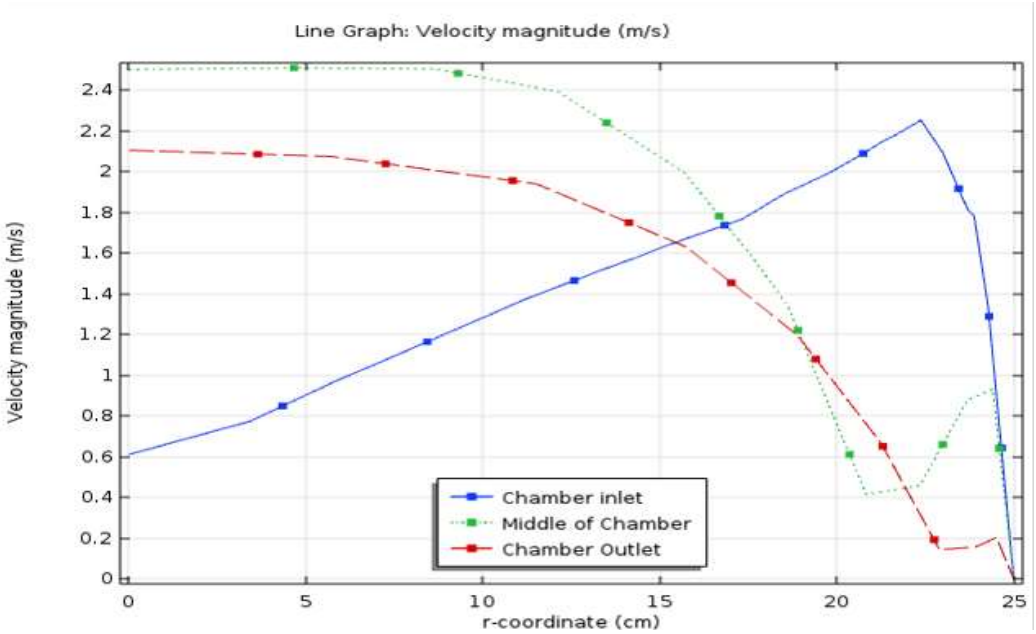

Fig. 3: 1D velocity profile in the drying chamber

It can be seen that the speed is high at the entrance to the chamber at the edge of the wall. This is due to the sudden change in the sensor outlet/drying chamber inlet section.
We observe that the velocity has a parabolic shape. We find that the speed is maximum in the middle of the drying chamber and practically zero near the wall of the drying chamber. This means that there is a boundary layer near the wall of the drying chamber. Indeed, the air pressure creates a longitudinal velocity which is canceled at the wall by the viscous effects.
Also, we find that the speed increases until the middle of the chamber (maximum value of 2.5 m/s) and then it decreases until the exit of said chamber (maximum value 2.1 m/s).

3.2 Pressure Profile

Figure 4 shows the evolution of air pressure in the solar dryer.

ISSN: 2277-9655
Impact Factor: 5.164
CODEN: IJESS7

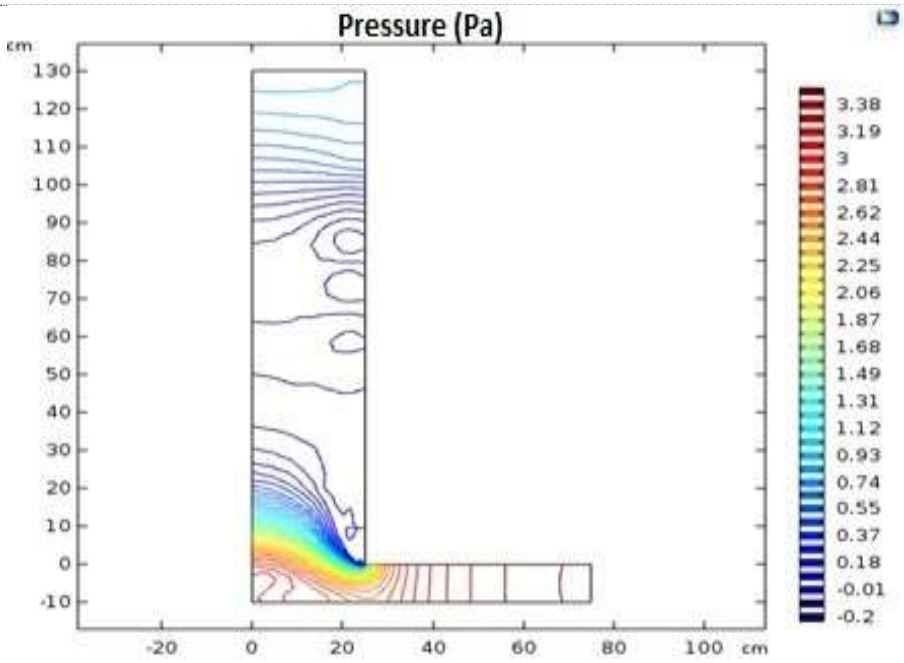

Fig. 4: 2D Pressure profile in the dryer

The pressure step is 0.10 Pa. We note that the pressure is relatively high in the plane sensor (around 2 Pa). It then decreases from the drying chamber inlet to the outlet, where it returns to atmospheric pressure. There is a minimum pressure value of -0.20 Pa in the middle of the drying chamber and a maximum value of 3.38 Pa at the beginning of the drying chamber.

3.3 Pressure-Velocity comparison

Figure 5 shows the evolution of pressure and speed along the drying chamber.

ISSN: 2277-9655
Impact Factor: 5.164
CODEN: IJESS7

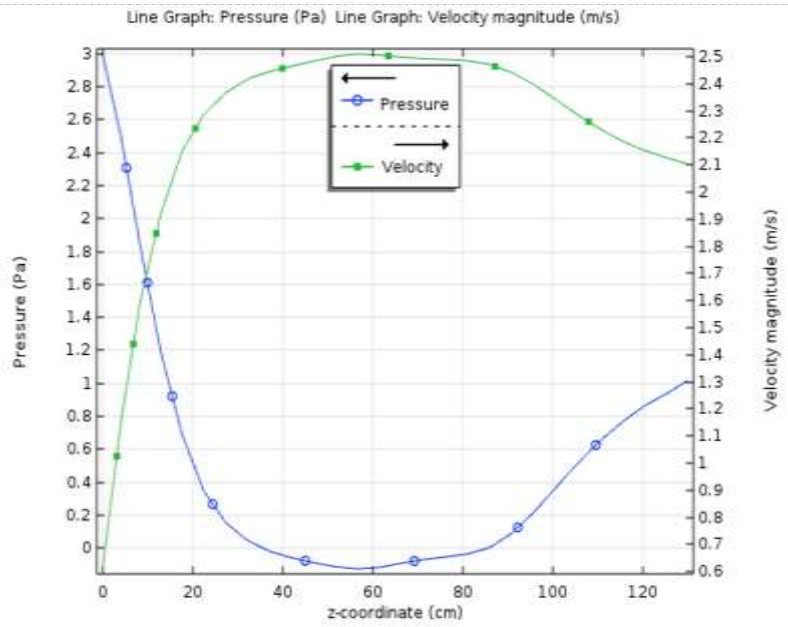

Fig. 5 : 1D velocity and pressure profile in the drying chamber

It is noted that the pressure and the air velocity evolve inversely in the drying chamber. From the entrance to the exit of the drying chamber, there is an increase in speed and simultaneously a decrease in pressure. Also, it is noted that the maximum value of the velocity (2.5 m/s) is reached in the middle of the drying chamber and the minimum value of the pressure (−0.20 Pa) is also reached at this level.

3.4 Temperature Profile

Figure 6 shows the 2D air temperature in the dryer.

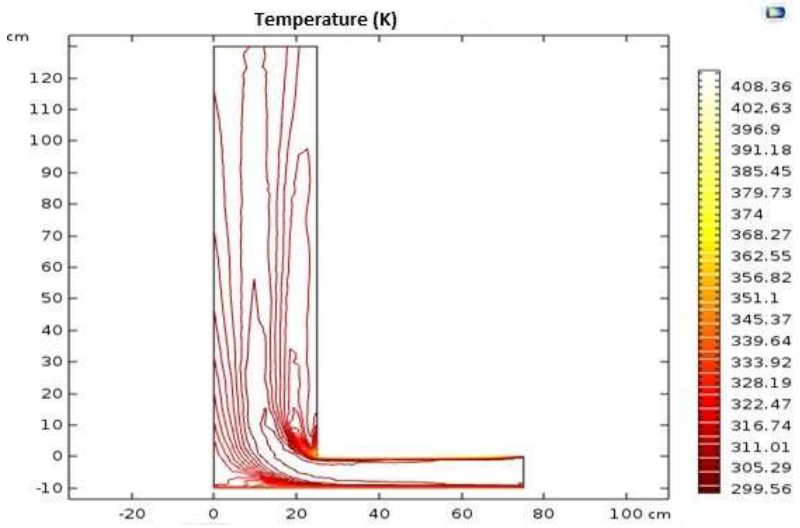

Fig. 6: 2D temperature profile in the dryer

Initially, the air temperature at the inlet of the collector is 303 K and that of the absorber is 343 K. We interpret this by the fact that the air is warmer in the vicinity of the absorber than near the glass. Indeed, the absorber absorbs more heat than a pane of glass. This causes a temperature increase of 19°C at the base of the drying chamber. Then, this temperature decreases to 303 K at the top of the drying chamber.
Thus, we have an air temperature in the drying chamber that varies from 322 K (at the base) to 303 K (at the top).

Figure 7 shows the 1D temperature profile along the drying chamber.

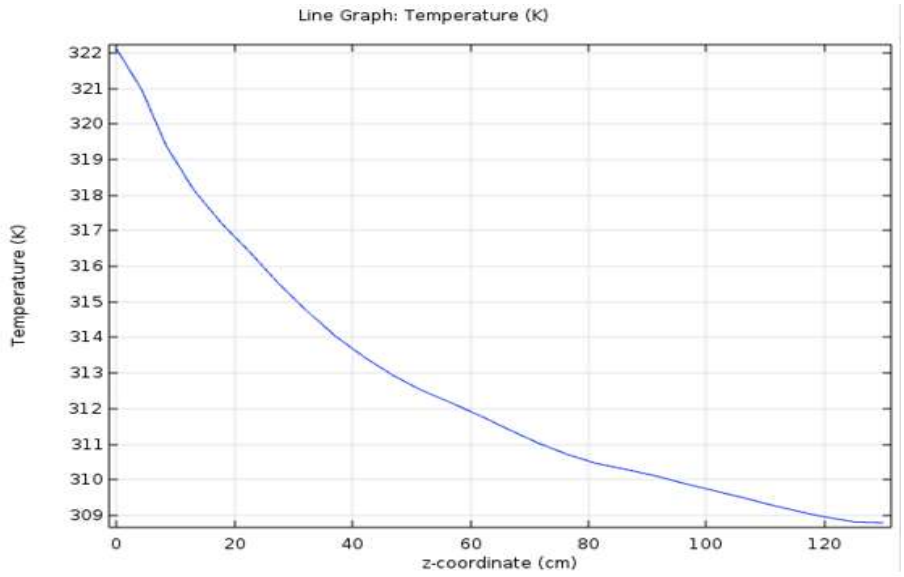

Fig. 7: 1D temperature profile in the drying chamber.

We find that the temperature increases from the entrance of the drying chamber to the exit. This means that the future products which will be placed in the drying chamber (on the racks) will dry in a decreasing manner, i.e. from bottom to top : the 1st rack will dry faster than the second rack placed just above and so on.
Also, we obtained temperatures that vary from 322 K to 310 K. This temperature range will make it possible to properly dry food products. Indeed, according to some authors, to better preserve the nutritional elements of agri-food products, the drying temperature should not exceed 60°C [9].

3.5 Influence of Dryer Diameter

Figures 9.a and 9.b show, respectively, the temperature and velocity profiles of the drying air for different radii: 40 cm, 50 cm, and 60 cm.

ISSN: 2277-9655
Impact Factor: 5.164
CODEN: IJESS7

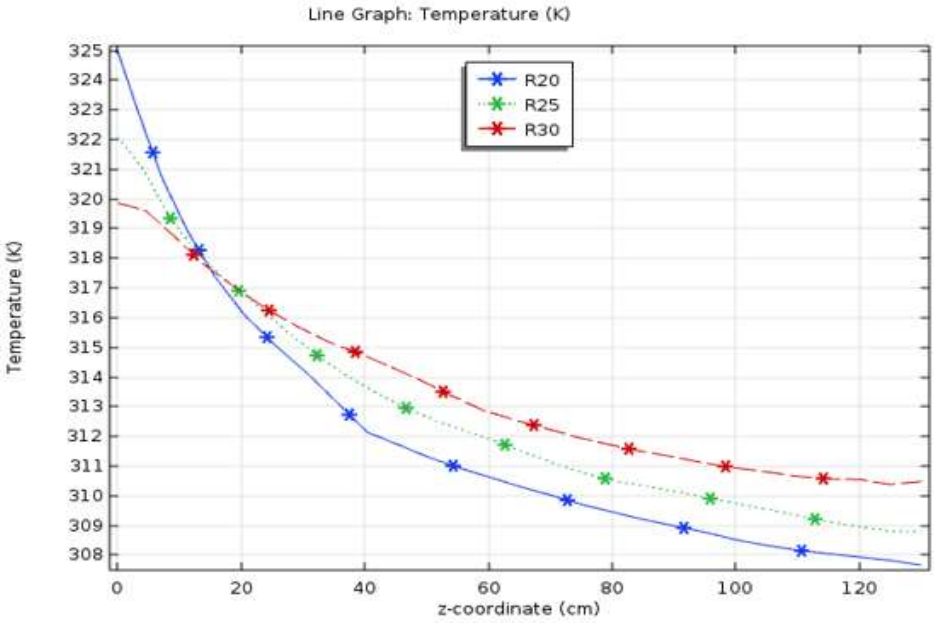

Fig. 9.a: Air temperature profile in the drying chamber for different radii

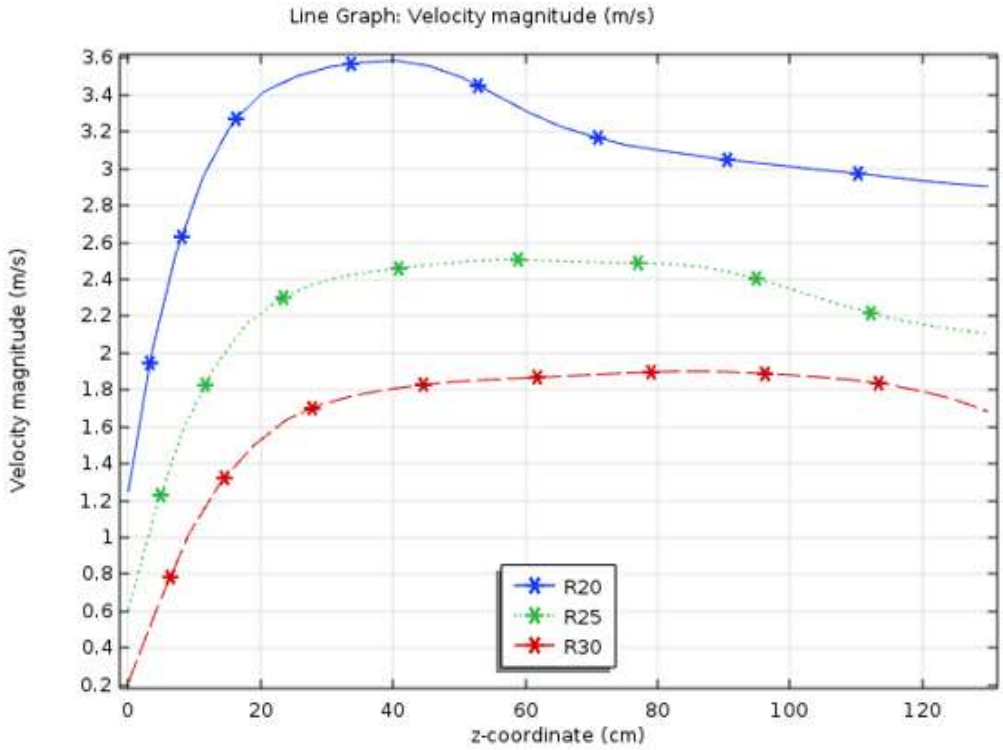

Fig. 9.b : Air velocity profile in the drying chamber for different radii

It can be seen that the greater the radius of the drying chamber, the more the temperature increases in the chamber. This result is in agreement with that of [10].

Also, it is found that an increase in the radius of the drying chamber leads to a decrease in the speed of the drying air inside the chamber. Indeed, an increase in the cross section of the air flow and therefore the mass flow rate causes a decrease in the flow velocity of this air. These same results have been reported by some authors such as [10] and [11].

4. CONCLUSION

We proceeded to the mathematical simulation of an indirect solar dryer. We have put into equation the phenomenon of air flow in laminar regime in a vacuum solar dryer. This is governed by the Navier-Stokes equations. The discretization of these equations, by a finite difference method, led to systems of algebraic equations that we solved using Gauss's algorithm.

We also studied the influence of the diameter of the solar dryer on the temperature and air velocity in the drying chamber. Also, it has been shown that increasing the radius of the drying chamber increases the mass of the airflow through the drying chamber.

The results obtained (temperature, speed and pressures), presented in the form of profiles, will make it possible to calculate the different energy quantities and more specifically the drying kinetics of agri-food products.

REFERENCES

[1] Gustavsson, J. et al. (2012). Pertes et gaspillages alimentaires dans le monde - ampleur, causes et prévention. In Congrès International SAVE FOOD. Organisation des Nations Unies pour l'Alimentation et l'Agriculture (FAO) Rome.

[2] Dagenet, M., 1985. "Les séchoirs solaires : théorie et pratique", UNESCO, 575 p.

[3] Dissa, A., E.,Tiendrebeogo, S., Garba, J., Koulidiati, 2016. "Modélisation et simulation du séchage solaire en couche mince de la Spiruline (Asthrospira platensis) ", J. Soc. Ouest-Afr. Chim., 042 : 1 – 7.

[4] El-Sebaii, A. A., S., Aboul-Enein, M. R. I., Ramadan and H. G., El-Gohary, 2002. "Experimental investigation of an indirect type natural convection solar dryer", Energy conversion and management 43, 2251-2266.

[5] Bejan, A., Convection Heat Transfer. John Wiley & Sons, New York, 1984

[6] Bouhdjar, A., Phénomène de stratification dans une cuve de stockage thermique - Etude paramétrique-. Thèse de Docteur d'Etat, Université de Tlemcen, 2005.

[7] Heisler E.M. (2014) Heisler, E. M., 2014. "Exploring alternative designs for solar chimneys using computational fluid dynamics". Master of science in mechanical engineering, faculty of the Virginia Polytechnic Institute Blacksburg, VA, 90 p.

[8] Amori K.E., Mohamed S.W., Experimental and numerical studies of solar chimney for natural ventilation in Iraq, Energy and Buildings 47(2012)450-457.

[9] Pendre, N.K. et al, (2011). Effect of drying temperature and slice size on quality of dried okra. Journal of Food Science and Technology.

[10] Maia, C.B., Ferreira, A.G., Vall, R.M., Cortez, F.B.M. (2009). Theoretical evaluation of the influence of geometric parameters and materials on the behavior of the airflow in a solar chimney. Computers and Fluids, 38(3): 625-636.

[11] Chergui, T., Bouhdjar, A., Larbi, S., Boualit, A. "Thermo-hydrodynamic Airflow Behavior Analysis in Solar Chimney Device", Periodica Polytechnica Mechanical Engineering, 66(4), pp. 289–303, 2022